

The nature of persistent conformational chirality, racemization mechanisms, and predictions in diarylether heptanoid cyclophane natural products†

Cite this: *Org. Biomol. Chem.*, 2014, **12**, 3303

Ommidala Pattawong, M. Quamar Salih, Nicholas T. Rosson, Christopher M. Beaudry* and Paul Ha-Yeon Cheong*

Restricted rotations of chemical bonds can lead to the presence of persistent conformational chirality in molecules lacking stereocenters. We report the development of first-of-a-kind predictive rules that enable identification of conformational chirality and prediction of racemization barriers in the diarylether heptanoid (DAEH) natural products that do not possess stereocenters. These empirical rules-of-thumb are based on quantum mechanical computations (SCS-MP2/∞//B3LYP/6-31G*/PCM) of racemization barriers of four representative DAEHs. Specifically, the local symmetry of ring B and the *E/Z* configuration of the vinylogous acid/ester are critical in determining conformational chirality in the DAEH natural product family.

Received 21st December 2013,
Accepted 4th April 2014

DOI: 10.1039/c3ob42550a

www.rsc.org/obc

Molecular chirality is of paramount importance to chemistry, biology, and medicine.¹ Small molecules that are chiral by virtue of restricted rotations (atropisomerism), or conformational chirality, are an underdeveloped territory with the potential for new developments of chiral ligands, medicinal compounds, catalysts, and materials. At present, there are no known methods to predict the presence of persistent conformational chirality in these compounds based solely on their molecular architecture without resorting to total synthesis.^{2,3} Specifically in this report, we have developed predictive rules-of-thumb for the chiral properties of all members in a family of cyclophane natural products called the diarylether heptanoids (DAEHs). Additionally, we elucidate the atomistic and energetic details related to the racemizations.

DAEHs are characterized by oxa[1.7]metaparacyclophane molecular architecture (Fig. 1).⁴ We (CMB and MQS) recently prepared the DAEHs that lack stereocenters and showed that some (but not all) are chiral.⁵ To the best of our knowledge, the presence of conformational chirality in these natural products cannot be predicted without resorting to total synthesis. In addition, determining the mechanism of racemization proved to be challenging even with the compounds in hand.

We believed that we could address both challenges through computations of four model DAEHs. The four model DAEHs are expected to be representative of similar members of the family because DAEHs that have similar structure type (*e.g.* the vinylogous acids) were found experimentally to have nearly identical racemization barriers.

We discovered that the complete stereoisomerization of a DAEH requires torsional rotations of all the stereogenic functional groups. The number of possible rotational sequences is equal to the factorial of the number of stereogenic groups in a given DAEH. Therefore, all intermediates and transition structures (TSS) for all possible sequences have been computed for each of the DAEHs discussed at SCS-MP2⁶/def2-∞⁷//B3LYP⁸/6-31G*⁹/PCM (dichlorobenzene)¹⁰ level of theory.¹¹

Of four representative DAEHs, acerogenin L most closely resembles the parent DAEH structure. There are two substituents: OH at C₂ and O at C₉. The complete racemization of acerogenin L requires the rotations of 3 stereogenic functional groups: C₇–C₈, C₉O, and C₁₁–C₁₂. There are a total of 3! (6) stereoisomerization pathways for acerogenin L; all were computed (Fig. 2B).

The minimum energy pathway for racemization is shown in Fig. 2 (A, B in black). Specifically, the sequence of rotation is: (i) C₁₁–C₁₂ ($\Delta G^\ddagger = 8.8 \text{ kcal mol}^{-1}$); (ii) C₉O ($\Delta G^\ddagger = 6.1 \text{ kcal mol}^{-1}$); (iii) C₇–C₈ ($\Delta G^\ddagger = 7.8 \text{ kcal mol}^{-1}$). The rate-determining step (RDS) is the C₁₁–C₁₂ rotation with a half-life ($t_{1/2}$) of $3.15 \times 10^{-7} \text{ s}$ at 25 °C (in the box, Fig. 2). From these barriers, we predict that acerogenin L is achiral – the enantiomeric conformations racemize rapidly under ambient conditions. The

Department of Chemistry, Oregon State University, 153 Gilbert Hall, Corvallis, Oregon 97331-4003, USA. E-mail: paulc@science.oregonstate.edu, christopher.beaudry@oregonstate.edu; Tel: +1 5417376760

† Electronic supplementary information (ESI) available: Coordinates, energies, additional figures, and full authorship of Gaussian. See DOI: 10.1039/c3ob42550a

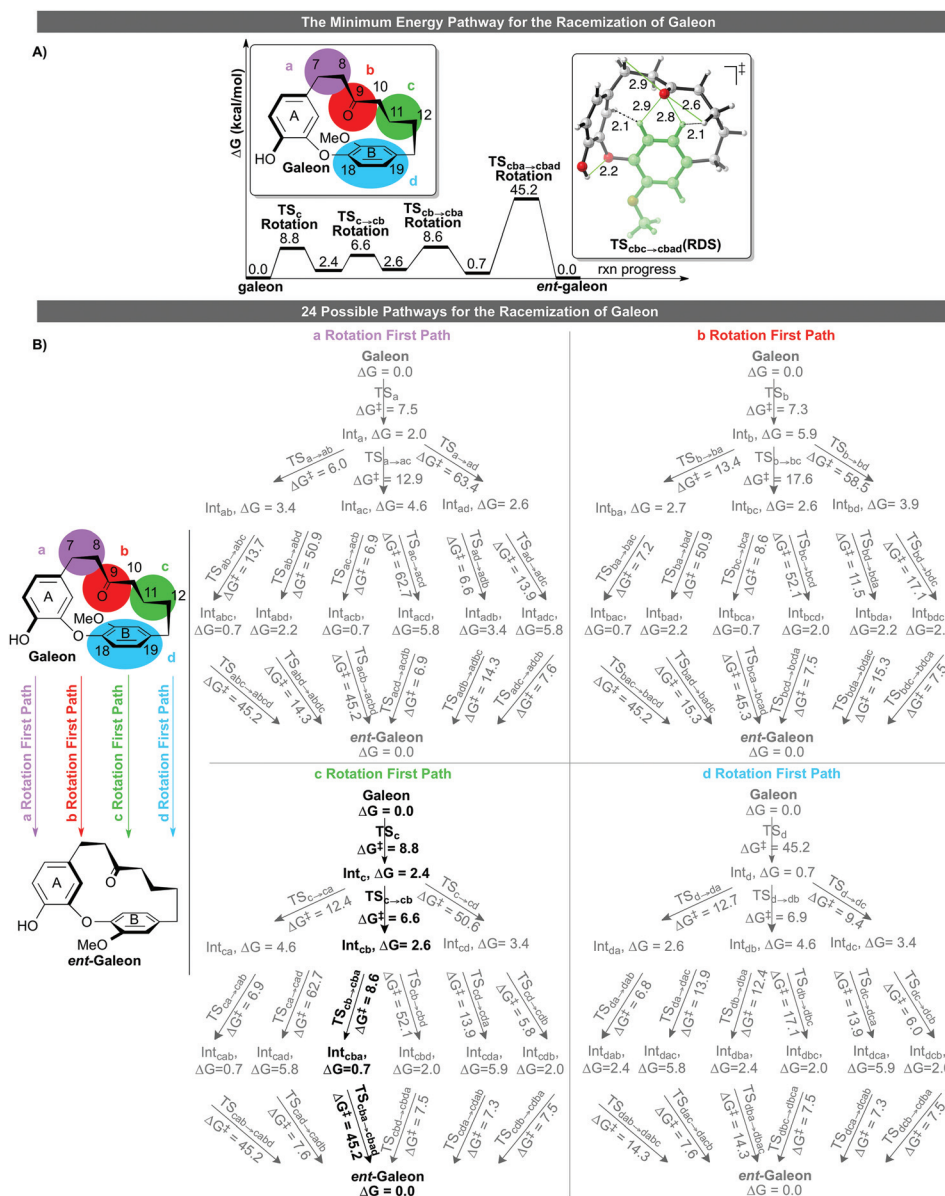


Fig. 3 (A) The minimum energy path and the RDS for racemization of galeon. (B) Twenty four possible racemization pathways.^{12,13}

Interestingly, 9'-desmethylgarugamblin I, possessing a vinylogous acid in the ansa chain has different ground state geometric preferences compared to garuganin III, with a vinylogous ester ansa chain.

There are a total of five tautomers of 9'-desmethylgarugamblin I (Fig. 4): keto, C₉-E, C₁₁-E, C₉-Z and C₁₁-Z. The designations C₉ and C₁₁ describe the position of the carbonyl, and Z/E define the stereochemistry of the vinylogous acid. The Z- are more stable than the E-isomers by ~8–10 kcal mol⁻¹, most likely due to the presence of stabilizing H-bonding interaction between the enol and the carbonyl. In fact, our model systems show that almost all the stability differences between the E- and the Z-tautomers arise from the stability of the intramolecular hydrogen bond in the Z-isomer (Fig. 5). The classical hydrogen bonding interactions present in the Z-isomer, is favored

over non-classical hydrogen bonding CH...O interactions present in E-isomers, by 8.6 kcal mol⁻¹.

There is a subtle energetic preference for the C₉-regioisomers compared to the C₁₁-regioisomeric vinylogous acid (~1–2 kcal mol⁻¹). We originally hypothesized that this is most likely due to the stronger CH...O interactions^{15,16} between H₆ and C₉ carbonyl O. Our model system study shows that the ketone oxygen and enol oxygen are similar hydrogen bonding acceptors (Fig. 6). We thus conclude that the majority of the energetic preference for the C₉/C₁₁ arises from subtle conformational and interaction changes from being constrained in a ring.

A total of 3! (6) stereoisomerization pathways for the C₉-E tautomers of 9'-desmethylgarugamblin I were computed. Surprisingly, only 3 pathways lead to the complete racemization

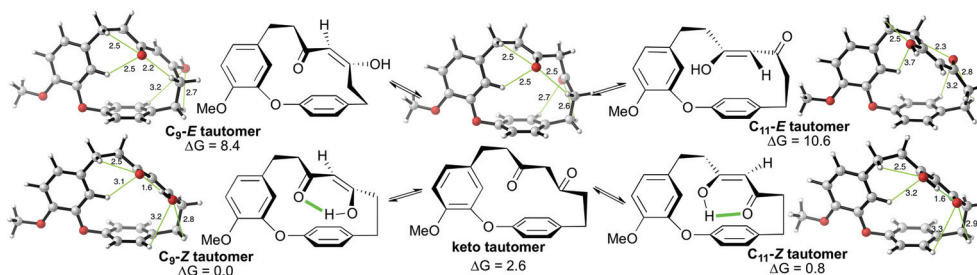


Fig. 4 Five tautomers of 9'-desmethylgarugambin I.^{13b}

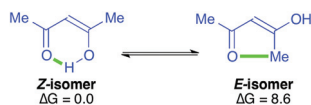


Fig. 5 Magnitude of stabilization from the intramolecular hydrogen bonding in 9'-desmethylgarugambin I.¹³

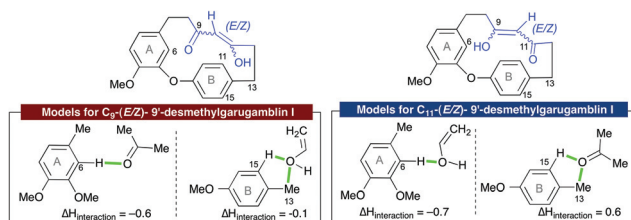


Fig. 6 Comparison of strengths of CH...O-ketone/enol interactions, and C₆H/C₁₅H...O interactions found in tautomers of 9'-desmethylgarugambin I.

(Fig. 7B). The introduction of an olefin in the ansa chain causes the barrier for functional group rotation to increase dramatically. In particular, TS_{b→ba}, TS_{b→bc} and TS_{c→cb} transition states caused the molecule to revert back (TS_{b→ba}) to the ground state or in the latter cases (TS_{b→bc} and TS_{c→cb}), these led to unproductive isomerization pathways that do not result in racemization due to coupled rotational motions of several functional groups.

The minimum energy pathway for racemization is shown in Fig. 7 (A, B in black). The sequence of rotation is: (i) C₁₀₋₁₃ ($\Delta G^\ddagger = 33.2 \text{ kcal mol}^{-1}$); (ii) C_{7-C8} ($\Delta G^\ddagger = 26.2 \text{ kcal mol}^{-1}$); (iii) C_{9O} ($\Delta G^\ddagger = 18.3 \text{ kcal mol}^{-1}$). The rate-determining step (RDS) is the C₁₀₋₁₃ rotation with a half-life ($t_{1/2}$) of $2.43 \times 10^{11} \text{ s}$ at 25 °C.

The complete racemization processes of the more stable C₉-Z tautomers of 9'-desmethylgarugambin I requires the rotations of 3 stereogenic functional groups: C_{7-C8}, C_{9-C10}, and C_{12-C13}. Theoretically, there should be a total of 3! (6) stereoisomerization pathways for C₉-Z tautomers. However, computations showed that the process of C_{9-C10} first rotation is simultaneous with the rotation of C_{12-C13}. Therefore, there are total of five stereoisomerization pathways for C₉-Z-9'-des-

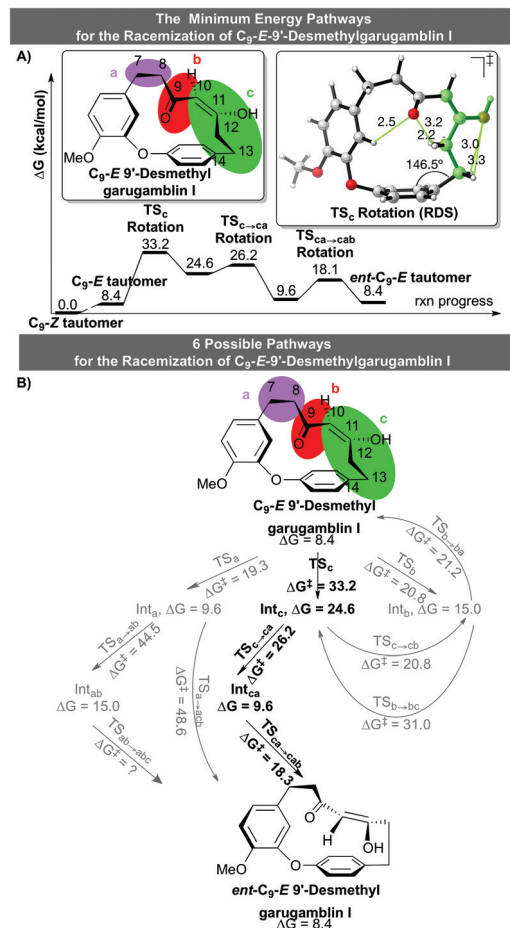


Fig. 7 (A) The minimum energy path and RDS for racemization of C₉-E-9'-desmethylgarugambin I. (B) Six possible racemization pathways.^{12,13}

methylgarugambin I (Fig. 8B). Interestingly, there are four equivalent minimum energy pathways found for this process (Fig. 8B in black). The representative minimum energy path is shown in Fig. 7A. The rotation of C_{12-C13} is found to be a common RDS for all minimum energy pathways with $\Delta G^\ddagger = 9.6 \text{ kcal mol}^{-1}$ or $t_{1/2} = 1.22 \times 10^{-6} \text{ s}$ at 25 °C. The predicted barrier at -80 °C is $8.8 \text{ kcal mol}^{-1}$, or $t_{1/2} = 1.56 \times 10^{-3} \text{ s}$. This value agrees well with the experimental data ($\Delta G^\ddagger = 9.1 \text{ kcal mol}^{-1}$ or $t_{1/2} = 3.3 \times 10^{-3} \text{ s}$ at -80 °C).

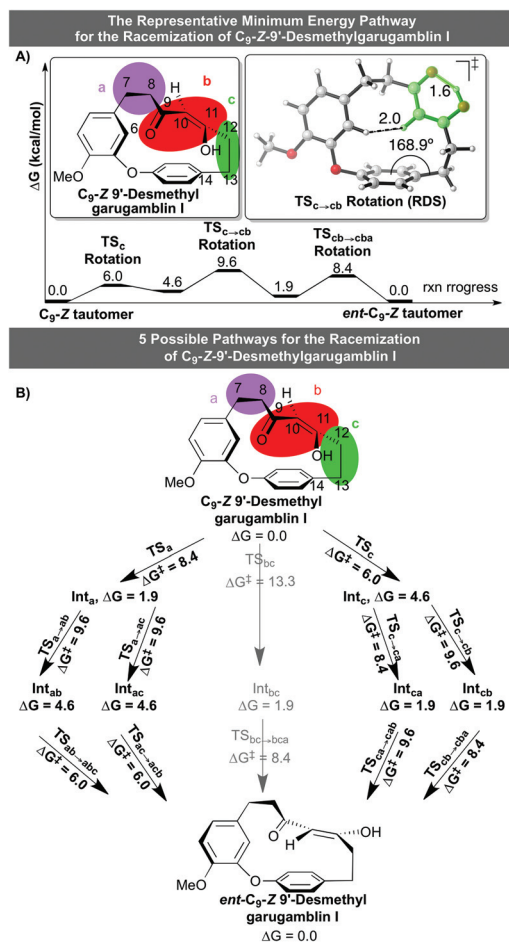


Fig. 8 (A) The representative minimum energy path and RDS for racemization of C_9 -Z-9'-desmethylgarugambin I. (B) Five possible racemization pathways.^{12,13}

Surprisingly, the racemization barrier of C_9 - E tautomer of 9'-desmethylgarugambin I is higher than the C_9 -Z by 23.6 kcal mol⁻¹ (Fig. 7 and 8, respectively). In effect, the C_9 - E vinylogous acids are locked in one regiomer and diastereomer conformation and undergo racemization with a higher barrier than the vinylogous acids, which can exist in the C_9 -Z configuration. This larger barrier comes from the geometric distortions sustained by the macrocycle in the E -isomer, as seen by the greater C_{14} out-of-plane distortion in the RDS (146.5° compared to 168.9°).

Since the keto-enol tautomers depicted in Fig. 4 are in equilibrium, the molecule will racemize *via* the reaction coordinate with lowest available transition state. The lowest barrier is the C_9 -Z tautomer. The calculated barrier corresponds closely with the experimental value.

Lastly, we investigated the vinylogous ester DAEHs. Specifically, garugambin I and its three vinylogous ester isomers were considered.¹⁷ Again, the designations C_9 and C_{11} describe the position of the carbonyl, and Z/E define the stereochemistry of the vinylogous ester. Unlike 9'-desmethylgarugambin I, the Z -stereoisomers of garugambin I are less stable

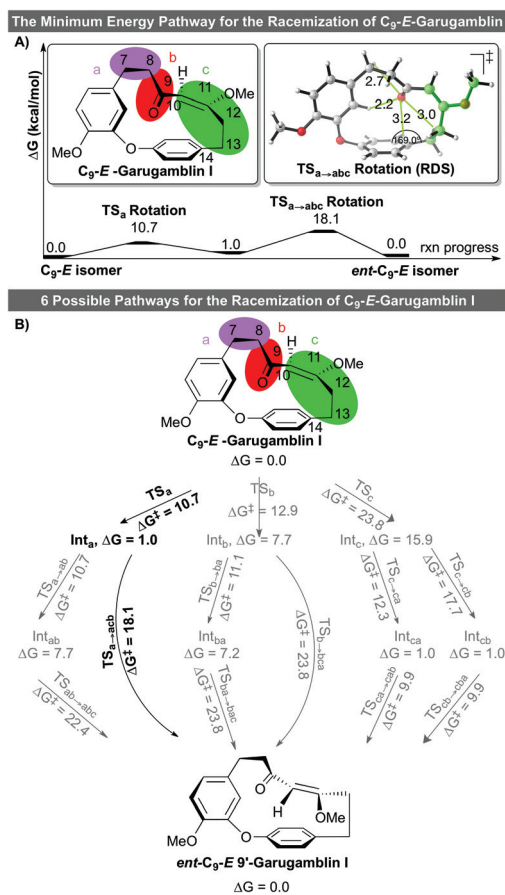


Fig. 9 (A) The minimum energy path and RDS for racemization of C_9 - E -garugambin I. (B) Six possible racemization pathways.^{12,13}

than the E by ~4–6 kcal mol⁻¹ due to the inherent steric repulsions in the Z -vinylogous ester. In fact, the Z -conformer is significantly distorted from planarity by ~20°. Similar to the 9'-desmethyl analogue, C_9 - E/Z tautomers are more stable than C_{11} - E/Z tautomers due to stronger CH...O interactions between H_6 and C_9O .

All stereoisomerization pathways for the C_9 -Z and C_9 - E isomers of garugambin I were computed. Interestingly, the minimum energy pathway for the racemization of C_9 - E isomer involves simultaneous rotations of C_9O and C_{10-13} (Fig. 9B in black). Consequently, the complete racemization of the C_9 - E isomer only requires two steps: C_7 - C_8 and C_{10-13} rotations. The C_{10-13} rotation is the RDS ($\Delta G^\ddagger = 18.1$ kcal mol⁻¹, $t_{1/2} = 2.1$ s at 25 °C, Fig. 9A). This value is consistent with the experimental value ($\Delta G^\ddagger = 16.9$ kcal mol⁻¹, $t_{1/2} = 3.0 \times 10^{-1}$ s at 25 °C). For the racemization of C_9 -Z isomer, the vinylogous ester rotation is the RDS ($\Delta G^\ddagger = 13.8$ kcal mol⁻¹, $t_{1/2} = 1.46 \times 10^{-3}$ s at 25 °C).¹⁷ We predict that garugambin I, isolated as the C_9 - E isomer, would racemize at room temperature on the time scale of seconds.

A total of 3! (6) pathways for complete racemization of C_{11} - E tautomer of garugambin I were computed (Fig. 10B). Two minimum energy pathways are found for this process. The representative of minimum energy pathways is shown in

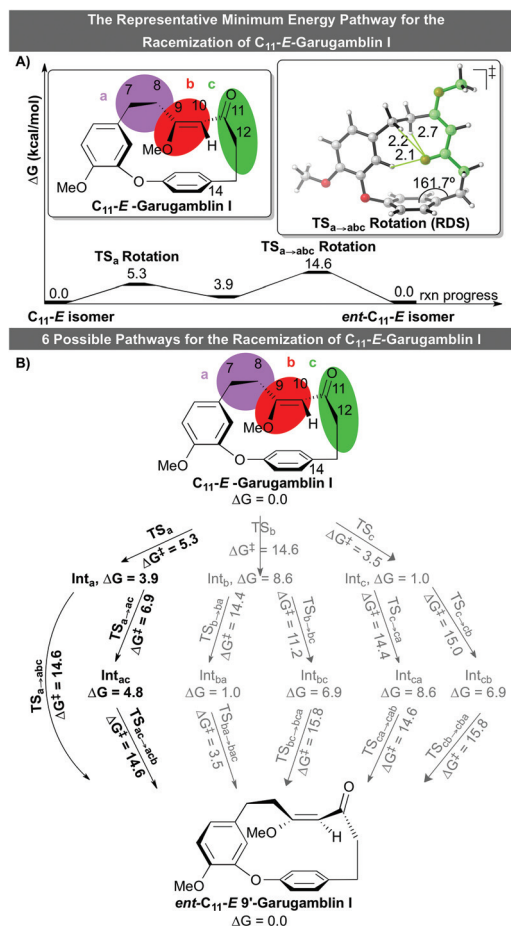


Fig. 10 (A) The representative minimum energy path and RDS for racemization of C_{11} -*E*-garugambin I. (B) Six possible racemization pathways.^{12,13}

Fig. 10A. Both asynchronous ($TS_{ab\rightarrow abc}$) and synchronous ($TS_{a\rightarrow abc}$) rotations of the vinylogous ester are the RDS with the barrier of 14.6 kcal mol⁻¹, or $t_{1/2} = 5.63 \times 10^{-3}$ s at 25 °C (at -10 °C, $\Delta G^\ddagger = 14.1$, or $t_{1/2} = 6.5 \times 10^{-2}$ s). The experimental values for the C_{11} -*E* tautomer of garugambin I are $\Delta G^\ddagger = 12.7$ kcal mol⁻¹, $t_{1/2} = 4.4 \times 10^{-3}$ s at -10 °C. Molecules with this structure type (such as garuganin III) undergo racemization rapidly at room temperature.

Conclusions

In conclusion, quantum mechanical computations predict the barriers of racemization for the four representative DAEHs in good agreement with experiments. These have led to the development of a predictive method that enables the identification of persistent conformational chirality and first order rules-of-thumb prediction of racemization barriers of all DAEHs that do not possess stereocenters (Fig. 11). The local symmetry of ring B and the *E/Z* configuration of the vinylogous acid/ester are critical in determining molecular conformational chirality in the DAEH natural product family.

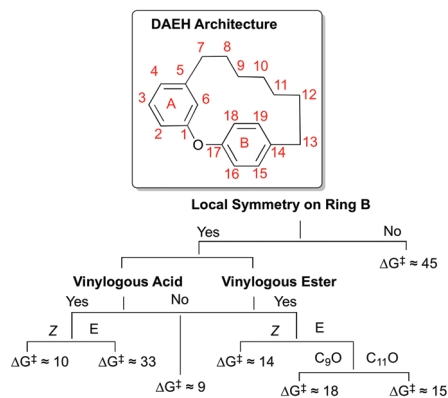


Fig. 11 Predicted barriers for racemization of conformational chirality of the four representative diarylether heptanoids used to deduce the data. ΔG^\ddagger are in kcal mol⁻¹.^{13b}

Notes and references

- 1 E. L. Eliel, S. H. Wilen and L. N. Mander, *Stereochemistry of Organic Compounds*, Wiley, 1994.
- 2 The chiral properties of acyclic diarylethers have been investigated, see: M. S. Betson, J. Clayden, C. P. Worrall and S. Peace, *Angew. Chem., Int. Ed.*, 2006, **45**, 5803.
- 3 Previously, molecular mechanics computational study of garuganin I using MMP2 force field suggested the molecule existed in single enantiomeric conformation at rt. see: A. Beyer, H. Kalchhauser and P. Wolschann, *Monatsh. Chem.*, 1992, **123**, 417. Experimentally, we found this to be inaccurate, see ref. 5b. Computational data presented in this work using quantum mechanics (SCS-MP2/B3LYP) agrees with experimental findings.
- 4 (a) S. Nagumo, S. Ishizawa, M. Nagai and T. Inoue, *Chem. Pharm. Bull.*, 1996, **44**, 1086; (b) K. E. Malterud, T. Anthonson and J. Hjortas, *Tetrahedron Lett.*, 1976, **35**, 3069; (c) J. Zhu, G. Islas-Gonzalez and M. Bois-Choussy, *Org. Prep. Proced. Int.*, 2000, **32**, 505; (d) P. Claeson, P. Tuchinda and V. Reutrakul, *J. Indian Chem. Soc.*, 1994, **71**, 509.
- 5 (a) M. Q. Salih and C. M. Beaudry, *Org. Lett.*, 2012, **14**, 4026; (b) Z.-Q. Zhu, M. Q. Salih, E. Fynn, A. D. Bain and C. M. Beaudry, *J. Org. Chem.*, 2013, **78**, 2881; (c) Z.-Q. Zhu and C. M. Beaudry, *J. Org. Chem.*, 2013, **78**, 3336; (d) M. Q. Salih and C. M. Beaudry, *Org. Lett.*, 2013, **15**, 4540; (e) M. Morihara, N. Sakurai, T. Inoue, K.-i. Kawai and M. Nagai, *Chem. Pharm. Bull.*, 1997, **45**, 820.
- 6 M. Gerenkamp and S. Grimme, *Chem. Phys. Lett.*, 2004, **392**, 229.
- 7 (a) A. Hellweg, C. Hättig, S. Höfener and W. Klopper, *Theor. Chem. Acc.*, 2007, **117**, 587; (b) S. Zhong, E. C. Barnes and G. A. Petersson, *J. Chem. Phys.*, 2008, **129**, 184116; (c) F. Neese and E. F. Valeev, *J. Chem. Theory Comput.*, 2011, **7**, 33.
- 8 A. D. Becke, *J. Chem. Phys.*, 1993, **98**, 5648.
- 9 (a) W. J. Hehre, R. Ditchfield and J. A. Pople, *J. Chem. Phys.*, 1972, **56**, 2257; (b) P. C. Hariharan and J. A. Pople, *Theor. Chim. Acta*, 1973, **28**, 213.

- 10 (a) PCM: S. Miertuš, E. Scrocco and J. Tomasi, *Chem. Phys.*, 1981, **55**, 117; (b) UFF: A. K. Rappé, C. J. Casewit, K. S. Colwell, W. A. Goddard III and W. M. Skiff, *J. Am. Chem. Soc.*, 1992, **114**, 10024.
- 11 This combination of methods has been used for high-accuracy computational studies of organic reactions. (a) O. Pattawong, T. J. L. Mustard, R. C. Johnston and P. H.-Y. Cheong, *Angew. Chem., Int. Ed.*, 2013, **52**, 1420; (b) M. D. Pierce, R. C. Johnston, S. Mahapatra, H. Yang, R. G. Carter and P. H.-Y. Cheong, *J. Am. Chem. Soc.*, 2012, **134**, 13624; (c) P. G. McGarraugh, R. C. Johnston, A. Martínez-Muñoz, P. H.-Y. Cheong and S. E. Brenner-Moyer, *Chem. – Eur. J.*, 2012, **18**, 10742; (d) O. Pattawong, D. Q. Tan, J. C. Fettinger, J. T. Shaw and P. H.-Y. Cheong, *Org. Lett.*, 2013, **15**, 5130.
- 12 C. Y. Legault, *CYLview 1.0b*, UCLA, Los Angeles, CA, 2007.
- 13 (a) The green highlighted atoms are directly involved in the transition state. Green lines indicate stabilizing hydrogen bonds and CH...O interactions; (b) Distances given in Å, energies in kcal mol⁻¹ and half-lives in seconds at 25 °C.
- 14 C. Rousel, A. Liden, M. Chanon, J. Metzger and J. Sandstrom, *J. Am. Chem. Soc.*, 1976, **98**, 2847.
- 15 (a) R. Hirschmann Jr., C. S. Snoddy and N. L. Wendler, *J. Am. Chem. Soc.*, 1952, **74**, 2693; (b) E. J. Corey, J. J. Rohde, A. Fischer and M. D. Azimioara, *Tetrahedron Lett.*, 1997, **38**, 33; (c) B. W. Gung, W. Xue and W. R. Roush, *J. Am. Chem. Soc.*, 2002, **124**, 10692; (d) R. S. Paton and J. M. Goodman, *Org. Lett.*, 2006, **7**, 4299; (e) S. Bahmanyar and K. N. Houk, *J. Am. Chem. Soc.*, 2001, **123**, 12911; (f) C. E. Cannizzaro and K. N. Houk, *J. Am. Chem. Soc.*, 2002, **124**, 7163.
- 16 R. C. Johnston and P. H.-Y. Cheong, *Org. Biomol. Chem.*, 2013, **11**, 5057.
- 17 Please see ESI.†